COMPARATIVE EFFECTS OF NATURAL POTASH (TRONA) AND SODIUM HYDROXIDE MERCERIZATION ON THE THERMAL STABILITY AND CRYSTALLINE STRUCTURE OF COCONUT COIR FIBER

MUHAMMED SANUSI,* JAMIU K. ODUSOTE** and KAMARDEEN O. ABDULRAHMAN*

*Department of Mechanical Engineering, Faculty of Engineering and Technology, University of Ilorin, Ilorin, Nigeria
**Department of Materials and Metallurgical Engineering, Faculty of Engineering and Technology, University of Ilorin, Ilorin, Nigeria
✉ Corresponding author: M. Sanusi, sanusi.m@unilorin.edu.ng

Received July 4, 2026

Coconut coir is an abundant lignocellulosic by-product whose use as a polymer-based composite reinforcement agent is hindered by the hydrophilic nature of its major components: cellulose and hemicelluloses, and by its surface layer of waxes and pectins, which prevent bonding with hydrophobic polymer matrices. Alkaline treatment (mercerization) with sodium hydroxide (NaOH) is the usual solution, but this reagent is produced by energy-intensive chlor-alkali electrolysis, leaving a strongly caustic effluent that must be neutralized before discharge. In this study, a locally sourced natural alkali traded in West Africa as "Kaun" was identified by X-ray diffraction as predominantly trona, $Na_3(CO_3)(HCO_3)\cdot 2H_2O$ (93 ± 2 wt%), and evaluated as a sustainable alternative to NaOH. Coir was mercerized at three concentrations (5, 10 and 20 g/dm³) for 4 h using both reagents, and characterized by attenuated-total-reflectance Fourier-transform infrared spectroscopy (ATR–FTIR), X-ray diffraction (XRD) and thermogravimetric analysis (TGA/DTG). FTIR showed that the acetyl C=O band of hemicelluloses at 1733 cm^{-1} was eliminated by both treatments, while the lignin bands at 1599 and 1509 cm^{-1} persisted, establishing that both reagents remove surface hemicelluloses selectively, without complete delignification. NaOH gave a higher crystallinity index (CrI) than trona at every concentration used, peaking at 27.5% at 10 g/dm³, causing over-mercerization at 20 g/dm³. The highest T_{max} (420 °C) occurred at 20 g/dm³ NaOH. The findings establish 10 g/dm³ NaOH as optimum and confirm trona as a viable natural alkali for coconut coir fiber treatment.

Keywords: coconut coir, mercerization, trona, sodium hydroxide, X-ray diffraction, thermogravimetric analysis, crystallinity index, natural fiber composites

INTRODUCTION

The accelerating global accumulation of synthetic plastic waste and the chronic underutilization of agricultural lignocellulosic residues have created a strong scientific incentive to develop polymer composites in which a portion of the petroleum-derived reinforcement is replaced by waste-stream natural fibers.[1,2] Coconut coir, the fibrous mesocarp of the coconut fruit, is one of the most widely produced agricultural by-products in tropical Africa and Asia, and is, on a weight basis, comparable in tensile strength to commodity glass fiber, while being significantly less dense, biodegradable, and effectively cost-free at source.[3,4] The interest in coir as a structural reinforcement has accordingly been growing, with recent studies reporting tensile-strength improvements of up to 42% in coir-reinforced epoxy composites after suitable surface treatment of the fiber.[5,6]

The principal obstacle to the effective use of coir, and indeed to all natural lignocellulosic fibers, is its hydrophilicity. The fiber surface carries a high density of free hydroxyl groups belonging to cellulose, hemicelluloses, and lignin, and is covered by a layer of waxes, pectins and mineral inclusions that obstruct mechanical interlocking and chemical bonding with hydrophobic polymer matrices, such as epoxy and polyester.[7,8] The resulting weak fiber matrix

interface limits stress transfer, lowers the apparent tensile and flexural strength of the composite, and renders the laminate susceptible to moisture-driven property degradation.[9,10] The accepted remedy is alkaline treatment, also referred to as mercerization, in which the fiber is immersed in a strong base for a controlled period of time. The alkali hydrolyses the acetyl ester linkages of the surface hemicelluloses, removes part of the lignin and waxes, increases the surface roughness, and partially converts the cellulose I crystal lattice toward cellulose II, all of which combine to expose a cleaner cellulosic surface for matrix bonding.[11,12]

Sodium hydroxide (NaOH) is the alkali most frequently reported in the natural-fiber composite literature, typically applied at concentrations between 2 and 10 wt% for soaking times of 1–6 h.[13] While the chemistry of NaOH-based mercerization is well characterized, and the reagent itself is inexpensive per kilogram at bulk industrial scale, its large-scale use is not without environmental and logistical cost. NaOH is manufactured by chlor-alkali electrolysis, a process whose life-cycle burden is dominated by the electricity consumed in the electrolysis cells;[39] the spent alkaline liquor is strongly caustic and requires neutralization before disposal; and, for fiber processors in sub-Saharan Africa, continued reliance on an imported chemical reagent carries a supply-chain and foreign-exchange exposure that sits awkwardly with the broader sustainability agenda that motivates the use of natural fibers in the first place.[14] There has therefore been growing interest in the use of locally available, evaporite-derived alkalis as substitutes for, or at least supplements to, NaOH in fiber treatment.[15]

In West Africa, a coarse alkaline mineral known in Yoruba as “Kaun”, and in Hausa as “kanwa” or “akanwu”, has been used for centuries in food preparation, traditional medicine, and indigenous textile processing. Although the material is colloquially translated as “potash” and assumed in much of the older literature to be a potassium-based salt dominated by K_2CO_3, recent work has shown that the lump form widely traded under the name “Kaun bilala” is in fact a sodium-based evaporite from the Lake Chad basin, with trona, $Na_3(CO_3)(HCO_3)\cdot 2H_2O$, as its principal phase.[16] This mineralogical reality is of direct relevance to mercerization chemistry. A trona-dominated alkali dissolves in water to give a buffered Na^+-carbonate/bicarbonate solution rather than a strongly basic K^+-hydroxide solution, and the cation in solution is therefore the same Na^+ as in dilute NaOH. The two reagents differ only in the counter-ion (CO_3^{2-}/HCO_3^- versus OH^-) and in the absolute hydroxide-ion activity delivered at a given mass concentration. This makes trona a natural candidate for direct, quantitative benchmarking against NaOH as a fiber-mercerizing reagent.

Three complementary analytical techniques are particularly informative when characterizing the effect of an alkaline treatment on a lignocellulosic fiber. Fourier-transform infrared (FTIR) spectroscopy reports directly on which chemical constituents of the fiber have been altered or removed, through the acetyl C=O ester band of hemicelluloses at ≈1733 cm^{-1}, the aromatic C=C ring stretches of lignin at ≈1600 and ≈1509 cm^{-1}, and the C–O–C glycosidic stretch of cellulose at ≈1030 cm^{-1}.[11] X-ray diffraction (XRD) provides a direct measure of the cellulose crystallinity index (CrI) and is the standard tool used to monitor the selective removal of amorphous hemicelluloses and the partial dissolution of disordered cellulose.[17] Thermogravimetric analysis (TGA) and its derivative (DTG) record the temperature, rate, and onset of each mass-loss step and are sensitive to the relative proportions of hemicelluloses (220–300 °C), cellulose (320–400 °C), and lignin (broad, above 200 °C) in the fiber.[18,19] A shift of the principal DTG peak to higher temperatures after treatment is widely accepted as a marker of improved thermal stability and of preferential surface enrichment in cellulose.[20] Used in combination, FTIR, XRD and TGA/DTG provide a chemical, crystallographic and thermal picture of the changes produced by the alkali.

Despite the abundance of NaOH-mercerization studies on natural fibers, there are very few that report a side-by-side comparison of a synthetic alkali and a locally derived natural alkali at identical concentration and exposure conditions, and fewer still that combine FTIR functional-group analysis, XRD-based crystallinity-index analysis and quantitative TGA/DTG on the same set of treated samples. The present work was therefore designed to address this gap. Coconut coir was mercerized in parallel using trona (Kaun bilala) and analytical-grade NaOH, each at three nominal concentrations (5, 10, and 20 g/dm^3) for a fixed soaking time of 4 h at room temperature, and the six treated batches were characterized by ATR–FTIR, XRD and TGA/DTG against the as-received raw fiber. The objectives were to (i) confirm the mineralogical identity of the natural potash, so that

the comparison with NaOH could be interpreted in terms of cation/counter-ion chemistry rather than vague "natural-versus-synthetic" categories, (ii) establish spectroscopically which fiber constituents each reagent removes, so that the crystallographic and thermal results could be referred to a direct record of compositional change, (iii) quantify the change in CrI produced by each reagent and concentration, (iv) quantify the corresponding change in the principal thermogravimetric markers (T_{max}, peak height, residue at 800 °C), and (v) identify the alkali and concentration that delivers the best combination of cellulose enrichment, increased crystallinity and preserved thermal stability for downstream composite manufacture.

EXPERIMENTAL

Raw materials

Coconut husks were obtained as agricultural waste from Odo Oba, Ogbomosho axis, Oyo State, Nigeria. The husks were retted in fresh water for seven days to soften the binding matrix, after which the fibers were extracted manually, washed in distilled water, oven-dried at 60 °C for 24 h, and stored in sealed polyethylene bags over silica gel to prevent moisture pickup. The dried fibers were cut to a uniform 20–30 mm length before treatment.

Lumps of natural potash were purchased from Oja-Oba market, Ilorin, where it is sold under the trade name "Kaun bilala". The material was ground in an agate mortar to a fine powder, sieved through a 150 µm mesh, and stored in a desiccator over silica gel. Analytical-grade sodium hydroxide pellets (≥99% purity) were obtained from a reputable chemical vendor and used as received. Distilled water was used as the solvent throughout.

Mercerization protocol

For each treatment, a fresh aqueous alkaline solution of 5, 10, or 20 g/dm³ was prepared in a 1 L beaker. Approximately 20 g of pre-weighed dried coir was immersed in 500 mL of the solution at room temperature (28 ± 2 °C) and held for 4 h with occasional gentle stirring. The 4 h duration was selected following the practice established in the coir-fiber literature, where treatment times of 1–6 h are reported to maximize delignification, without compromising fiber integrity.[5,12] After treatment, each batch was thoroughly rinsed with distilled water until the rinsing water was neutral to litmus, and oven-dried at 60 °C for 24 h.

The six treated batches were coded throughout this work as A, B and C for the trona-treated coir at 5, 10 and 20 g/dm³, respectively, and as E, F and G for the NaOH-treated coir at the same three concentrations. The untreated raw fiber is denoted RC throughout.

X-ray diffraction

X-ray diffraction patterns were recorded on a Rigaku MiniFlex benchtop diffractometer (Rigaku Corporation, Tokyo, Japan), operated with Cu Kα radiation (λ = 1.5406 Å) at 30 kV and 15 mA. Each sample was scanned over the 2θ range 5–70°, at a step size of 0.02° and a counting time chosen to give a good signal-to-noise ratio. The cellulose crystallinity index (CrI) was calculated from the diffractogram using the Segal two-point method given in Equation (1):

$$CrI(\%) = \left(\frac{I_{200} - I_{am}}{I_{200}}\right) \times 100 \quad (1)$$

where I_{200} is the maximum intensity of the (200) crystalline reflection at 2θ ≈ 22°, and I_{am} is the minimum intensity associated with the amorphous fraction at 2θ ≈ 18°.[21,22] To suppress high-frequency counting noise, every profile was smoothed using a five-point Savitzky–Golay filter before peak picking. The reagent powder (Kaun) itself was also characterized over the same 2θ range, and quantitative phase composition was extracted by Rietveld refinement using the diffractometer software.

Fourier-transform infrared spectroscopy

The functional groups of the raw and mercerized fibers were examined by attenuated-total-reflectance Fourier-transform infrared (ATR–FTIR) spectroscopy on an Agilent Cary 630 spectrometer (Agilent Technologies, USA), fitted with a diamond ATR accessory. Finely chopped fiber was pressed directly onto the crystal with the anvil to ensure uniform optical contact, and spectra were recorded from 4000 to 650 cm^{-1} at a spectral resolution of 4 cm^{-1} with 32 co-added scans per spectrum. A background spectrum was collected on the clean diamond surface immediately before each sample, so that any instrumental drift was compensated for. The diagnostic bands monitored were the broad hydrogen-bonded O–H stretch near 3350 cm^{-1}, the aliphatic C–H stretch near 2900 cm^{-1}, the acetyl C=O ester of hemicelluloses at 1733 cm^{-1}, the aromatic C=C ring stretches of lignin at 1599 and 1509 cm^{-1}, and the C–O–C glycosidic stretch of cellulose at 1028 cm^{-1}.[11]

Thermogravimetric analysis

Thermal stability was assessed on a PerkinElmer TGA 4000 thermogravimetric analyzer (PerkinElmer Inc., USA). For each measurement, 5–10 mg of the sample was placed in a platinum pan and heated from 30 °C to 800 °C at 10 °C/min under a nitrogen flow of 100 mL/min. Three parameters were extracted from each TG/DTG curve, the onset degradation temperature (T_{onset}), the temperature of maximum rate of mass loss (T_{max}), and the residual char content at 800 °C, all of which are widely used as indicators of fiber quality and the effectiveness of any surface treatment.[23,24]

RESULTS AND DISCUSSION

Identification of the natural alkali

Because the natural alkali used in this study is a locally produced reagent of variable composition, its chemical and crystallographic identity was verified before any treatment work was undertaken. The XRD diffractogram of the Kaun powder, recorded over 2θ = 5–70°, is composed entirely of sharp, intense crystalline reflections riding on a near-zero baseline, in sharp contrast to the broad amorphous halo of the raw coir reported in the next section in this study. Quantitative phase analysis by Rietveld refinement returned the phase composition listed in Table 1: trona (trisodium hydrogen dicarbonate dihydrate, $Na_3(CO_3)(HCO_3)\cdot 2H_2O$) at 93 ± 2 wt%, sylvite (KCl) at 1.7 ± 0.3 wt%, and muscovite ($KAl_2(Si_3Al)O_{10}(OH,F)_2$) at 5 ± 2 wt%. The diffractogram is presented in Figure 1.

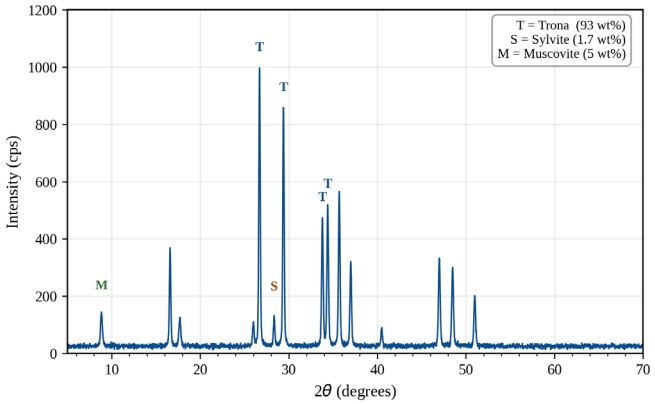


Figure 1: X-ray diffractogram of the natural alkali (Kaun bilala) recorded over 2θ = 5–70° – the pattern is dominated by sharp crystalline reflections attributable to trona (T, 93 wt%), with minor sylvite (S) and muscovite (M)

Table 1
Phase composition of the natural alkali (Kaun bilala) as determined by Rietveld refinement of the XRD pattern

Phase	Chemical formula	Composition (wt%)
Trona	$Na_3(CO_3)(HCO_3)\cdot 2H_2O$	93 ± 2
Sylvite	KCl	1.7 ± 0.3
Muscovite	$KAl_2(Si_3Al)O_{10}(OH,F)_2$	5 ± 2

This finding is a major chemically important observation in the present work and requires careful discussion. In Yoruba and Hausa markets across West Africa, the local term Kaun is widely translated into English as "potash". It is consequently assumed in much of the literature to be a potassium-based salt dominated by K_2CO_3. The Rietveld result obtained here, however, demonstrates unambiguously that the Kaun used in this study is sodium-based, with trona accounting for 93 wt% of the crystalline material. Trona is a hydrated, mixed sodium carbonate–bicarbonate mineral that occurs as an evaporite in alkaline lake beds. The most prominent African source is the Lake Chad basin, and the material excavated from these deposits is widely traded across the Sahel under the trade name Kaun bilala ("the Kaun from Bilala", after the Kanem–Bornu region near Lake Chad).[16,25] The presence of small amounts of sylvite (KCl, the only true potassium phase detected) and detrital muscovite is fully consistent with the mineralogy of an evaporite of this kind.

This mineralogical identification has two immediate consequences for the comparison reported in subsequent sections. First, because trona is sodium-based and dissolves in water to give a Na^+-carbonate/bicarbonate solution, the cation delivered to the fiber surface during mercerization is the same Na^+ as in dilute NaOH. The comparison between the two reagents, therefore, reduces to a comparison between two counter-ions (CO_3^{2-}/HCO_3^- versus OH^-) at the same Na^+ concentration, rather than a poorly constrained comparison between two different alkali metals. Second, at the concentrations used here (5, 10, and 20 g/dm³), the practical alkalinity delivered by trona is substantially lower than that delivered by NaOH at the same mass concentration, because trona is a buffered carbonate system whose dissociation does not

produce free hydroxide ion at the same stoichiometric ratio as NaOH. This is precisely the chemical distinction between a "mild natural alkali" and a "strong synthetic alkali" that the present study sets out to evaluate.

Baseline crystallinity of the raw fiber

The XRD diffractogram of the as-received coir is dominated by a single broad reflection centred at 2θ ≈ 22° with a maximum intensity of approximately 1020 counts per second (cps), and a clear amorphous minimum at 2θ ≈ 18° with an intensity of about 600 cps (Fig. 2). This profile is the classical fingerprint of cellulose I, the native crystalline allomorph found in all higher-plant lignocellulosic fibers, in which the (200) planes of the hydrogen-bonded cellulose chains diffract at ≈ 22°, while the disordered, amorphous fraction contributes a baseline minimum near 18°.[26,27] A second sharp reflection at 2θ ≈ 26.6° with an intensity of approximately 460 cps is too narrow and too well-defined to be of organic origin and is best assigned to crystalline silica (α-quartz), consistent with previous reports of natural silica inclusions in coconut husks.[28,29]

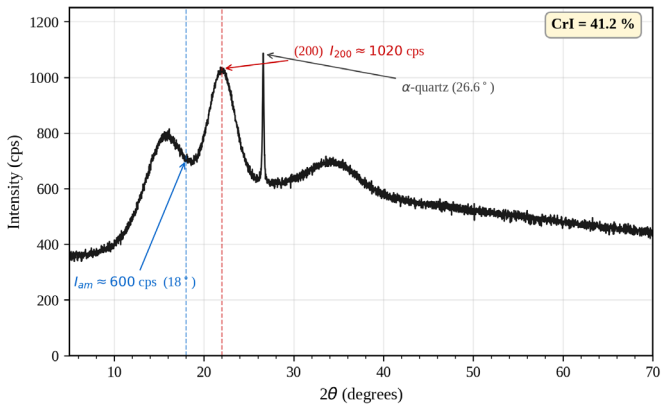


Figure 2: X-ray diffractogram of raw (untreated) coconut coir fiber over 2θ = 5–70°

The application of the Segal two-point method (Eq. 1) to the raw fiber with I_{200} ≈ 1020 cps and I_{am} ≈ 600 cps gives CrI ≈ 41.2%. This value places the present coir largely within the range reported in the literature for untreated coconut coir (32–50%), which typically depends on cultivar, retting conditions and the analytical method adopted.[28] The relatively modest CrI reflects the high lignin and hemicellulose content of coir (cellulose 27–50 wt%, lignin 30–45 wt%, hemicelluloses 15–25 wt%), both of which are predominantly amorphous and therefore depress the apparent crystalline fraction.[30,31] This baseline value of CrI ≈ 41% is the explicit benchmark against which the change in cellulose crystallinity following mercerization is quantified in the next section.

Crystallinity index of mercerized fiber

The stacked XRD diffractograms of the six mercerized samples are presented in Figure 3, with the trona group (A, B, C) in panel (a) and the NaOH group (E, F, G) in panel (b). The diffractogram of every treated sample retains the cellulose-I fingerprint, namely the broad (200) reflection centered near 22° and the less-resolved shoulder near 15°, indicating that none of the six treatments transforms the cellulose lattice into the cellulose-II allomorph. This is consistent with the relatively mild conditions used here (room temperature, 4 h, ≤20 g/dm³) compared with the high-concentration, long-duration treatments (≥17 wt% NaOH, >12 h) required to drive the cellulose I → II transformation.[32]

The Segal-derived crystallinity indices of the six mercerized samples and the raw-fiber baseline are summarized in Table 2.

Within the trona group, the CrI values of Samples A, B and C are 22.4%, 19.9% and 22.2% respectively, indicating that increasing the trona concentration from 5 to 20 g/dm³ produces no steady gain in crystallinity and that, within experimental scatter, the three trona treatments are essentially equivalent in their effect on the cellulose crystal fraction. Sample B is marginally lower than the other two; this is consistent with the picture of a controlled, mild surface treatment in which the bulk crystallinity of the fiber is largely preserved and the alkali acts predominantly on the outer hemicellulose- and lignin-rich layer rather than penetrating the cellulose crystallites

themselves. The buffered carbonate/bicarbonate chemistry of trona, by limiting the free hydroxide-ion activity available for nucleophilic attack on the fiber, ensures that even at 20 g/dm³ the alkali concentration is below the threshold required to disrupt the cellulose lattice.

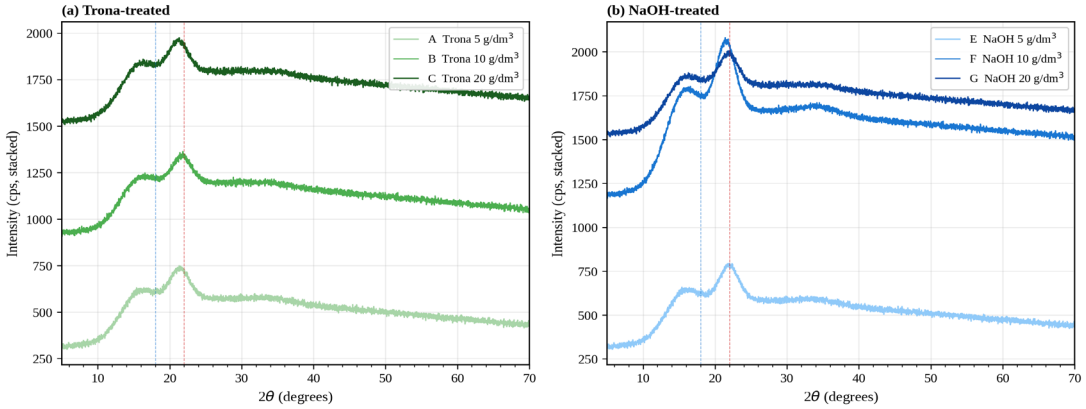


Figure 3: XRD diffractograms of the six mercerized coir samples: (a) trona-treated group (A: 5 g/dm³, B: 10 g/dm³, C: 20 g/dm³), and (b) NaOH-treated group (E: 5 g/dm³, F: 10 g/dm³, G: 20 g/dm³); vertical dashed lines mark the (200) crystalline peak (22°) and amorphous minimum (18°) used in the Segal calculation

Table 2
Crystallinity index of raw fiber and six mercerized coir samples obtained from XRD, using the Segal two-point method

Sample	Alkali	Conc. (g/dm³)	I_{200} (cps) [2θ°]	I_{am} (cps) [2θ°]	CrI (%)
RC	None	—	1020 [22.00]	600 [18.00]	41.2
A	Trona	5	733 [21.39]	569 [17.83]	22.4
B	Trona	10	737 [21.71]	591 [17.59]	19.9
C	Trona	20	758 [21.22]	590 [17.52]	22.2
E	NaOH	5	781 [21.95]	578 [17.78]	26.0
F	NaOH	10	1454 [21.51]	1054 [17.64]	27.5
G	NaOH	20	789 [21.87]	605 [18.21]	23.3

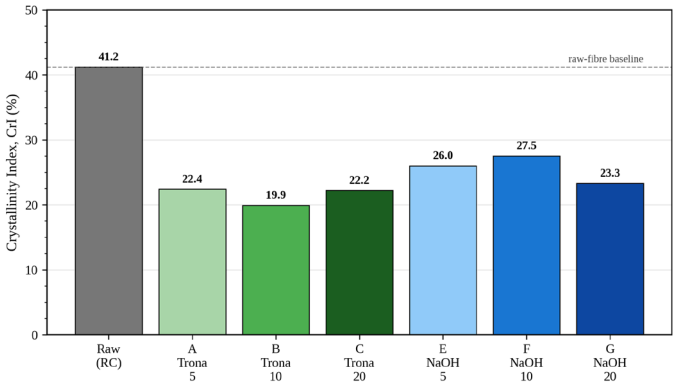


Figure 4: Comparison of the cellulose crystallinity index (CrI) of raw fiber (RC) and six mercerized coir samples (the horizontal dashed line marks the raw-fiber baseline (CrI = 41.2%))

The NaOH group shows a markedly different behaviour. The (200) reflection is consistently sharper and slightly better separated from the amorphous halo than in the trona group, and the CrI values are higher: 26.0%, 27.5%, and 23.3% for Samples E, F, and G, respectively. The trend rises from 5 to 10 g/dm³ and then falls back to 20 g/dm³, with Sample F (NaOH 10 g/dm³) returning the highest CrI of any treated sample in the study. The 27.5% maximum at moderate NaOH concentration is consistent with the classical interpretation of mercerization, in which a

moderate concentration of free hydroxide ion selectively dissolves amorphous hemicelluloses and the disordered fraction of the cellulose, raising the relative proportion of crystalline cellulose, without yet attacking the crystallites themselves.[32,33]

The drop from Sample F (CrI = 27.5%) to Sample G (CrI = 23.3%) at 20 g/dm³ NaOH is the spectroscopic and crystallographic signature of over-mercerization, in which the free hydroxide-ion activity has risen to a level that begins to penetrate and partially dissolve the cellulose crystallites that earlier, milder treatments had been enriching. Such a CrI response to increasing alkali concentration has been reported repeatedly in the literature for both flax and jute, and it is generally taken as the signal that the treatment has passed the point of diminishing returns and is starting to compromise the very phase it was intended to expose.[32,34] The trona group, by contrast, never reaches the over-mercerization regime, even at its highest concentration, because the buffered carbonate equilibrium of trona caps the free hydroxide activity well below the concentration at which crystallite dissolution becomes appreciable.

Comparing the two alkalis at matching concentrations, NaOH yields a higher CrI than trona at every one of the three concentrations tested: 26.0 versus 22.4% at 5 g/dm³, 27.5 versus 19.9% at 10 g/dm³, and 23.3 versus 22.2% at 20 g/dm³. This pattern is consistent with the cation-and-counter-ion analysis discussed above: trona and NaOH deliver the same Na^+ cation, but very different free hydroxide activities, and it is the free hydroxide that drives both the desirable removal of amorphous hemicelluloses and, at high concentration, the undesirable dissolution of cellulose crystallites.

Two observations regarding the absolute CrI values in Table 2 warrant explicit attention. First, none of the six mercerized samples reaches the raw-fiber baseline of CrI ≈ 41%. This is the opposite of the trend usually reported for mild alkali treatments of natural fibers, where mercerization typically raises CrI by selectively dissolving amorphous hemicelluloses. The most plausible explanation is methodological rather than physical: the diffractograms of the treated samples are noticeably noisier than the raw-fiber scan, and the Segal two-point method is known to be highly sensitive to the choice of the I_{am} baseline on broad cellulose halos.[35] Using a different baseline window or replacing the Segal method with a full peak-deconvolution analysis would be expected to shift the absolute CrI values upward; however, the relative ranking of the six samples, which is the discrimination required for selecting the optimum treatment, would be unlikely to change. Second, even at face value, the trend within the NaOH group (rise to a maximum at 10 g/dm³ followed by a fall at 20 g/dm³) and the consistent trona-versus-NaOH ordering at matched concentrations are internally consistent with the TGA evidence reported further in the study, and therefore reinforce, rather than undermine, the optimum-selection conclusion of this work.

Functional-group composition of raw and mercerized fibers

A full wet-chemical fractionation of the fiber into cellulose, hemicelluloses, lignin, extractives and ash was outside the analytical scope of the present study, but the compositional change produced by each treatment was followed spectroscopically, so that the crystallographic results discussed above and the thermal results in the next section could be referred to a direct, band-by-band record of which fiber constituents the alkali had removed. The ATR–FTIR spectra of the raw coir and the six mercerized samples are stacked in Figure 5, and the positions and transmittance minima of the six diagnostic bands are collected in Table 3.

The raw-fiber spectrum is a typical spectrum of lignocellulose. The broad hydrogen-bonded O–H stretch at 3336 cm^{-1} (88.4%T) and the aliphatic C–H stretch at 2903 cm^{-1} (93.3%T) are accompanied by a clearly resolved acetyl C=O ester band at 1733 cm^{-1} (94.8%T), the single most sensitive spectroscopic marker of unmodified hemicelluloses; by the aromatic C=C pair at 1606 and 1509 cm^{-1} that constitutes the lignin fingerprint; and by the strongest absorption of the spectrum, the C–O–C glycosidic stretch of the cellulose backbone at 1028 cm^{-1} (73.1%T). The raw fiber therefore carries exactly the hemicellulose- and lignin-rich surface layer that mercerization is intended to remove, which is the compositional counterpart of the modest baseline crystallinity of 41.2% reported above.

The most important observation in Table 3 is that the 1733 cm^{-1} acetyl band is absent from all six treated spectra, irrespective of reagent or concentration. Both the buffered carbonate alkalinity of trona and the free hydroxide of NaOH are therefore sufficient, at room temperature and 4 h, to hydrolyse the acetyl ester linkages of the surface xylan and to strip the accessible

hemicelluloses from the fiber.[11,12] This provides the compositional explanation for the thermogravimetric behavior reported in the next section. In an untreated lignocellulosic fiber, the 220–300 °C region of the DTG curve is dominated by hemicellulose decomposition; once that fraction has been removed, the principal mass-loss event is governed by cellulose and the DTG peak migrates into the 370–420 °C window. The 45 °C rise in T_{max} between Samples A and B, and the 420 °C maximum recorded for Sample G are therefore not isolated thermal observations, but the thermal expression of a compositional change that Figure 5 records directly.

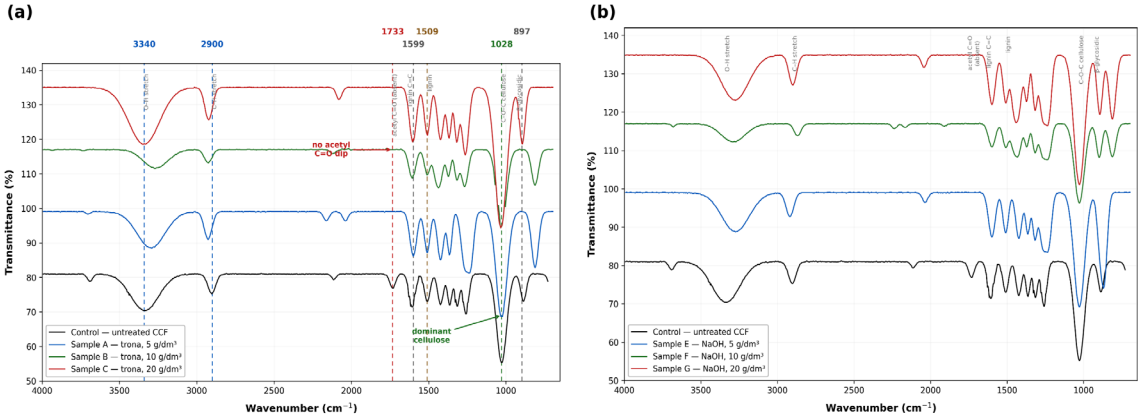


Figure 5: ATR–FTIR transmittance spectra of coir samples mercerized with (a) natural alkali trona (A: 5 g/dm³, B: 10 g/dm³, C: 20 g/dm³), and (b) synthetic NaOH (E: 5 g/dm³, F: 10 g/dm³, G: 20 g/dm³), each shown against the untreated raw fiber (control); vertical markers identify the acetyl C=O band of hemicelluloses (1733 cm⁻¹), the aromatic C=C bands of lignin (1599 and 1509 cm⁻¹) and the C–O–C glycosidic band of cellulose (1028 cm⁻¹)

Table 3
Positions (cm⁻¹) and transmittance minima (%T, in parentheses) of the principal FTIR bands of raw fiber and six mercerized coir samples

Sample	O–H stretch	C–H stretch	Acetyl C=O (hemicelluloses)	Lignin C=C	Lignin C=C	Cellulose C–O–C
Raw coir	3336 (88.4)	2903 (93.3)	1733 (94.8)	1606 (89.2)	1509 (90.8)	1028 (73.1)
A, trona 5 g/dm³	3295 (88.5)	2926 (91.0)	absent	1599 (86.1)	1509 (87.0)	1028 (68.1)
B, trona 10 g/dm³	3265 (93.6)	2926 (95.2)	absent	1606 (90.7)	1509 (91.7)	1028 (77.9)
C, trona 20 g/dm³	3340 (82.5)	2922 (89.6)	absent	1602 (83.0)	1509 (84.9)	1032 (58.2)
E, NaOH 5 g/dm³	3273 (88.8)	2918 (92.7)	absent	1599 (87.3)	1509 (88.3)	1028 (69.0)
F, NaOH 10 g/dm³	3287 (94.3)	2868 (95.8)	absent	1599 (92.9)	1509 (92.8)	1028 (78.2)
G, NaOH 20 g/dm³	3276 (87.2)	2899 (91.1)	absent	1599 (85.9)	1509 (86.5)	1028 (64.9)

The lignin bands behave differently from the hemicellulose band. The aromatic C=C pair near 1599–1606 and 1509 cm⁻¹ survives every treatment, so that neither reagent delignifies the fiber completely under the mild conditions used here; what changes is the depth of these bands, which increases with reagent concentration in both groups, from 87.0 %T at 1509 cm⁻¹ in Sample A to 84.9 %T in Sample C, and from 88.3%T in Sample E to 86.5%T in Sample G. Partial, concentration-dependent delignification of this kind is consistent with the known capacity of both hydroxide and carbonate alkalinity to cleave lignin–carbohydrate ester linkages, without dissolving the condensed lignin network.[11,33]

The cellulose-defining C–O–C band at 1028 cm⁻¹ provides the clearest link to the crystallinity data discussed in the section above. Its

transmittance minimum deepens from 73.1%T in the raw fiber to 68.1 and 58.2%T in Samples A and C of the trona group, and to 69.0 and 64.9%T in Samples E and G of the NaOH group, indicating a progressive enrichment of the surface in cellulose as the amorphous hemicelluloses and part of the lignin are removed. Samples B and F are the exceptions, each showing a shallower absorption envelope than its 5 g/dm³ counterpart. Because this shallowing affects the O–H, C–H, lignin and cellulose bands simultaneously rather than selectively, it is most plausibly a baseline effect arising from residual sample moisture or from variable ATR contact pressure on the day of measurement, rather than a chemical inversion of the concentration trend, although a localized re-deposition of dissolved cellulose oligomers during washing cannot be entirely excluded.[12] The spectroscopic ranking of the fiber surfaces is therefore broadly consistent with, but not identical to, the CrI ranking of Table 2, which is to be expected: ATR–FTIR examines only the outermost micrometre or two of the fiber, whereas the Segal crystallinity index is a bulk-averaged quantity.

Two limitations of this spectroscopic route to composition should be stated explicitly. First, the transmittance minima in Table 3 are semi-quantitative. They rank the samples reliably and identify unambiguously which constituent has been removed, but they do not return weight fractions. Second, no gravimetric fractionation of the present fiber batch, whether by the sequential neutral- and acid-detergent procedure[41] or by the corresponding TAPPI protocols, was undertaken; the cellulose, lignin and hemicellulose contents quoted for coir in this study are therefore literature values,[30,31] and not measurements on this material. A quantitative compositional analysis of the raw and optimally treated fiber, which would allow the CrI and T_{max} changes reported here to be converted into absolute mass balances of hemicellulose and lignin removal, is accordingly identified as the first priority of the follow-on work outlined further in the paper.

Thermal stability of mercerized fiber

The thermogravimetric analyses provide an independent check on the XRD-based interpretation because the relative amounts of cellulose, hemicelluloses, and lignin in a lignocellulosic fiber are directly reflected in the temperatures, sharpness, and heights of its mass-loss steps.[19] Three principal stages are typically observed in the TGA/DTG curves of plant-derived fibers: a low-temperature dehydration step (50–150 °C), the main decomposition stage (200–500 °C) in which hemicelluloses break down first (around 220–300 °C), followed by cellulose (320–400 °C), and finally lignin over a broad range, and a slow char-loss stage above 500 °C.[36,37] The corresponding DTG curve provides a clearer view of these stages, as each mass-loss event appears as a discrete peak. The principal numerical parameters extracted from the TGA/DTG curves of the six mercerized samples are collected in Table 4.

Trona-treated samples

All three trona-treated samples lose around 4% of their mass in the dehydration step below 150 °C and remain essentially stable until the onset of the main decomposition.

Table 4
Summary of TGA/DTG parameters for the six mercerized coir samples

Sample	Alkali	Conc. (g/dm³)	T_{max} (°C)	DTG peak height (%/min)	Residue at 800 °C (%)
A	Trona	5	370	−4.7	~25
B	Trona	10	415	−4.3	~7
C	Trona	20	330	−8.4	~10
E	NaOH	5	390	−3.5	~6
F	NaOH	10	380	−5.3	~16
G	NaOH	20	420	−4.7	~5

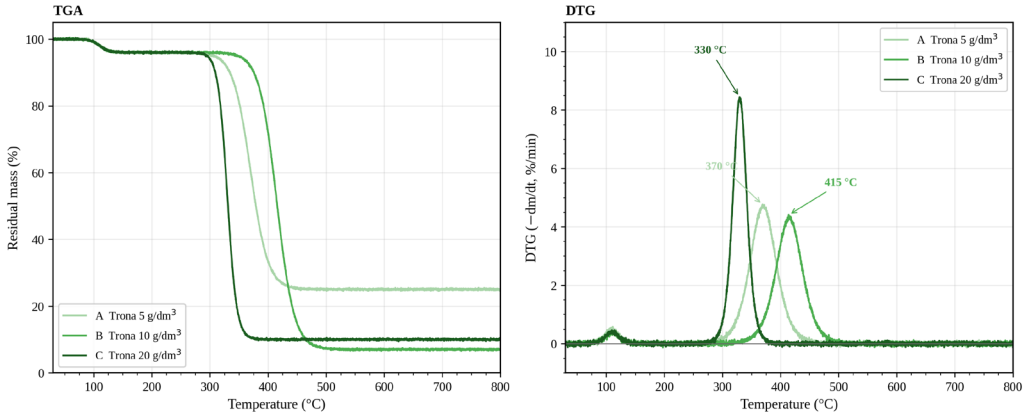


Figure 6: (Left) TGA and (right) DTG curves of trona-treated coir samples A (5 g/dm³), B (10 g/dm³) and C (20 g/dm³) recorded from 30 to 800 °C at 10 °C/min under flowing nitrogen

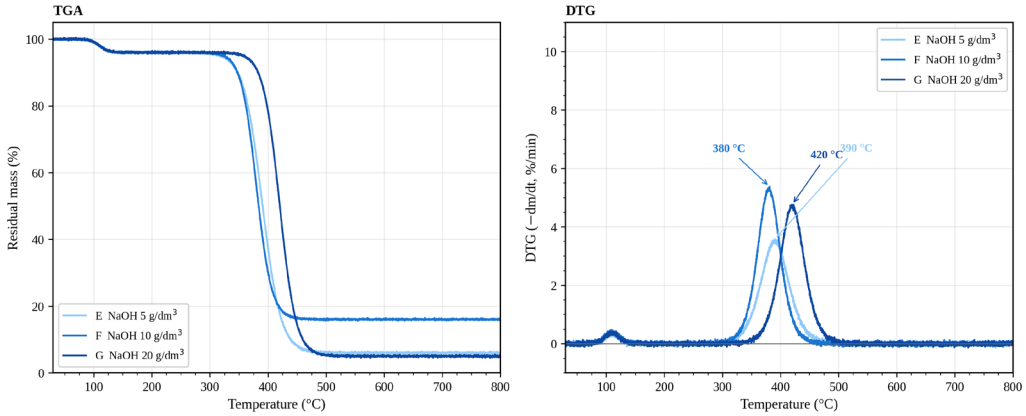


Figure 7: (Left) TGA and (right) DTG curves of NaOH-treated coir samples E (5 g/dm³), F (10 g/dm³) and G (20 g/dm³) under the same heating programme as in Figure 6

The most informative differences appear in the position and shape of the principal DTG peak. Sample A (5 g/dm³) shows a single, moderately broad DTG minimum at 370 °C with a peak height of 4.7 %/min, Sample B (10 g/dm³) shifts the peak to a markedly higher temperature of 415 °C, while reducing the peak height to 4.3 %/min, and Sample C (20 g/dm³) displays a much sharper and lower-temperature peak at 330 °C with the deepest DTG value of the entire study (−8.4 %/min). The 45 °C shift of T_{max} from 370 °C in Sample A to 415 °C in Sample B is a recognized marker of improved thermal stability and is widely interpreted as evidence that hemicelluloses, which decompose earliest, have been removed, while cellulose, which decomposes at higher temperature, has been enriched at the surface.[36,38] Sample B is therefore the most thermally stable of the trona group.

The behavior of Sample C is more complex and deserves further attention. Its DTG peak is extremely sharp, narrower, and deeper than in any other sample in this study, but it is centered at a lower temperature than the peaks of either Sample A or Sample B. This combination is most plausibly explained by recognizing that the high-concentration trona treatment has not only removed the hemicelluloses and a portion of the lignin, but has also begun to attack the more accessible amorphous cellulose itself, leaving behind a residue whose principal mass-loss event is dominated by a comparatively narrow population of cleavable bonds. Such over-mercerization effects have been reported with both concentrated NaOH and K_2CO_3 at high alkalinity.[12] The residue of Sample A at 800 °C is also unusually high (~25%) compared with Samples B (~7%) and C (~10%); this is most likely a consequence of incomplete removal of inorganic carbonate residues left behind when trona-treated coir is rinsed, since trona itself is a carbonate-based mineral and any incomplete washing can leave Na_2CO_3 deposits that resist thermolysis at high temperatures.

NaOH-treated samples

The thermograms of the NaOH-treated group exhibit a more linear and easier-to-interpret behaviour. The DTG peak of Sample E (5 g/dm³) is located at 390 °C with a height of 3.5 %/min, Sample F (10 g/dm³) shifts it slightly to ~380 °C with a deeper peak of 5.3 %/min, and Sample G (20 g/dm³) shifts it further to 420 °C with a peak of 4.7 %/min. The most thermally stable sample of the NaOH group is therefore Sample G, whose T_{max} of 420 °C is the highest of any sample in the study, including those treated with trona. Although T_{max} dips slightly from 390 °C at 5 g/dm³ (Sample E) to 380 °C at 10 g/dm³ (Sample F), it rises to the highest value of the entire study, 420 °C, at 20 g/dm³ (Sample G). This net increase in T_{max} at the highest NaOH concentration is consistent with the trend that NaOH at higher concentrations produces the most cellulose-enriched surface, and is in line with the morphological evidence reported elsewhere that NaOH at 20 g/dm³ is the most aggressively etched of the six samples.

Char residues at 800 °C for the NaOH group span 5% (Sample G) to 16% (Sample F). The intermediate residue value for Sample F is the most likely cause of the slightly anomalous behavior observed in that sample and reinforces the importance of standardized post-treatment rinsing in any future scaling-up of the procedure.

Cross-comparison and selection of the optimum treatment

Reading Tables 2 and 4 together, the optimum treatment must be selected on the basis of a multi-criteria comparison. The highest T_{max} of the entire experiment is achieved by Sample G (NaOH 20 g/dm³, 420 °C), narrowly followed by Sample B (trona 10 g/dm³, 415 °C). The highest CrI is achieved by Sample F (NaOH 10 g/dm³, 27.5%), while the trona group is led by Sample C (22.2%) and Sample A (22.4%). Sample F therefore offers the most favorable balance of high CrI and high thermal stability (T_{max} = 380 °C, CrI = 27.5%), and is selected as the overall optimum NaOH treatment. Sample G, despite reaching the highest T_{max}, is disqualified by the loss of crystallinity (CrI = 23.3%) that signals the onset of over-mercerization.

Within the trona group, the most favorable balance is achieved by Sample B (CrI = 19.9%, T_{max} = 415 °C), which delivers thermal stability close to that of the best NaOH treatment, but at a CrI that is approximately 8 percentage points lower. The lower crystallinity is a direct consequence of the buffered, mild alkalinity of trona and is therefore an intrinsic limitation of the natural reagent rather than a deficiency that can be addressed by raising the concentration: increasing trona to 20 g/dm³ produces no further gain in CrI and, as shown by the anomalous DTG peak of Sample C, may begin to attack the accessible amorphous cellulose. The clear practical recommendation is therefore that 10 g/dm³ NaOH should be used where the highest CrI is required (for instance, when the cellulose-rich surface is to be coupled to a polar matrix or used as a base for subsequent silane treatment), while 10 g/dm³ trona is the recommended natural-alkali alternative where the priority is sustainability and where a modest reduction in CrI can be accepted in exchange for a locally sourced, lower-impact reagent.

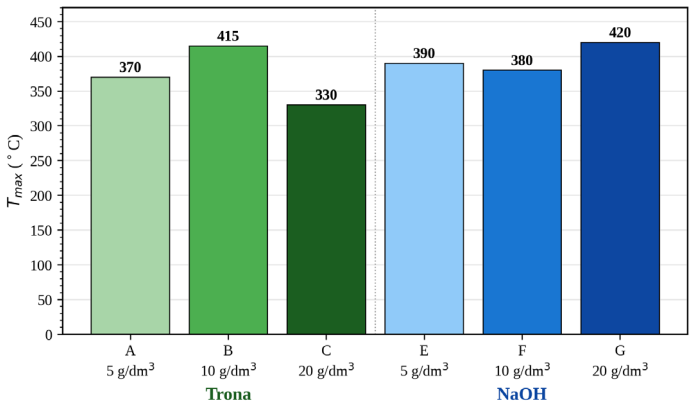


Figure 8: Comparison of the temperature of maximum mass-loss rate (T_{max}) extracted from the DTG curves of the six mercerized coir samples

A second, broader observation that emerges from the cross-comparison concerns the practical alkalinity delivered by the two reagents. At every matched concentration, NaOH outperforms trona by margins (3.6, 7.6 and 1.1 percentage points of CrI at 5, 10 and 20 g/dm³, respectively) that are roughly consistent with the difference in free hydroxide-ion activity between a fully dissociated hydroxide and a buffered carbonate/bicarbonate equilibrium. The trona–NaOH gap is widest at the intermediate concentration (10 g/dm³), where the NaOH treatment is at its most effective and the trona treatment is still well below its own ceiling, and narrowest at the highest concentration, where NaOH has already begun to over-mercerize and trona has reached an internal plateau. This pattern suggests that the locally sourced reagent could in principle be brought closer to NaOH-equivalent performance by raising the alkalinity in another way, for example by partial substitution with a small fraction of NaOH or by heating the bath, although such modifications would partially undermine the sustainability argument that motivates the use of trona in the first place.

Environmental and practical considerations in the choice of alkali

The case of replacing NaOH with a locally sourced natural alkali is often stated in general terms, and it is worth setting out explicitly what that case does and does not rest on. Sodium hydroxide is inexpensive at bulk industrial scale, and its low unit cost is one of the principal reasons for its dominance in natural-fiber treatment; the argument advanced here is therefore not that NaOH is an expensive reagent per kilogram. It rests instead on three narrower considerations. First, chlor-alkali production is electricity-intensive, and life-cycle analyses of the process identify the electricity consumed in the electrolysis cells as the dominant contributor to its climate-change, acidification and eutrophication burdens;[39] where that electricity is generated largely from fossil fuels, as it is on the West African grid, the embodied impact of the delivered reagent is correspondingly higher. Second, the spent liquor from caustic mercerization is strongly alkaline at the concentrations used here and requires neutralization before discharge, whereas the spent trona liquor is a buffered carbonate/bicarbonate solution of markedly lower pH and lower neutralization demand. Third, for a small-scale fiber processor in Nigeria, technical- or analytical-grade NaOH is a purchased and largely imported input, whereas Kaun bilala is available in every major market at low cost and without foreign-exchange exposure.

Against this, the environmental credentials of the natural alkali should not be overstated, and the impact of extracting and using the mineral deserves explicit comment. Trona and the associated natron evaporites traded as Kaun are obtained from the interdunal depressions and lake-margin playas of the Lake Chad basin, largely by manual or semi-mechanized surface excavation of the efflorescent crust, followed by solar evaporation and drying. The energy input of this route is very low: it involves no electrolysis, no chlorine co-product and no high-temperature processing, which is the principal reason to expect a lower cradle-to-gate burden than for synthetic NaOH. The extraction nevertheless takes place within a hydrologically stressed and ecologically sensitive Sahelian wetland system whose open-water extent and groundwater balance have changed substantially over recent decades,[40] and the natron workings occupy the same interdunal depressions that support local grazing, date cultivation and shallow-aquifer recharge. Unregulated artisanal excavation disturbs these surfaces, and the material must then be moved some 1500 km overland from the Lake Chad basin to the coconut-producing belt of southern Nigeria, so that road transport is likely to represent a non-trivial fraction of the delivered footprint of the reagent. In addition, the carbonate rinse water, although far less caustic than spent NaOH liquor, carries a dissolved sodium load that should not be discharged untreated onto cultivated soil.

The honest conclusion is therefore comparative and qualified rather than absolute. Trona is expected to carry a lower production-stage burden than NaOH because it is a directly obtained evaporite rather than an electrochemical product, and it yields a milder effluent; but its extraction is not impact-free, and its transport burden is real. No cradle-to-gate life-cycle assessment of either reagent, as delivered to a Nigerian fiber processor, was carried out in the present study, and the environmental comparison made here should be read as a reasoned qualitative argument rather than a quantified one. A comparative life-cycle assessment of the two mercerization routes, with inventory data collected from the Lake Chad natron supply chain and from the Nigerian chlor-alkali import chain, is identified as a necessary complement to the materials-science results reported above.

CONCLUSION

Coconut coir fiber was mercerized in parallel using a locally sourced natural alkali, identified by Rietveld refinement of XRD data as predominantly trona ($Na_3(CO_3)(HCO_3)\cdot 2H_2O$, 93 ± 2 wt%), and analytical-grade NaOH, each at 5, 10 and 20 g/dm³ for 4 h at room temperature. The crystalline and thermal effects of the six treatments were assessed by XRD-based crystallinity index (CrI) analysis and TGA/DTG measurement, against the as-received raw fiber as baseline. The principal findings are summarized below.

(1) The natural alkali traded in West African markets as Kaun bilala was unambiguously identified as a sodium-based evaporite dominated by trona, not the potassium-based potash that the colloquial name implies. This mineralogical clarification reduces the trona–NaOH comparison to a comparison between two counter-ions (CO_3^{2-}/HCO_3^- versus OH^-) at the same Na^+ cation, and therefore allows the chemistry of the two reagents to be discussed on a quantitative footing.

(2) Both reagents successfully mercerized the fiber under the conditions used, as evidenced by the complete disappearance of the 1733 cm^{-1} acetyl C=O band of hemicelluloses from every treated fiber FTIR spectrum and by the systematic shift of the principal DTG peak to higher temperatures; the lignin bands at 1599 and 1509 cm^{-1} persisted in all six samples, showing that neither reagent fully delignifies the fiber under these conditions. NaOH was, however, the more aggressive of the two, yielding a higher CrI than trona at every matched concentration.

(3) Within the NaOH group, the CrI rose from 26.0% at 5 g/dm³ to a maximum of 27.5% at 10 g/dm³ and fell back to 23.3% at 20 g/dm³, the latter accompanied by morphological and thermogravimetric evidence of over-mercerization in which the alkali begins to disrupt the cellulose crystallites that lower concentrations had been enriching.

(4) Within the trona group, the three concentrations returned essentially equivalent CrI values in the 19.9–22.4% range, consistent with a controlled, mild treatment in which the buffered carbonate chemistry caps the free hydroxide activity below the over-mercerization threshold.

(5) The highest thermal stability (T_{max} = 420 °C) was recorded for the 20 g/dm³ NaOH treatment, narrowly followed by the 10 g/dm³ trona treatment (415 °C). The most favorable overall balance of crystallinity and thermal stability was returned by the 10 g/dm³ NaOH treatment (CrI = 27.5%, T_{max} = 380 °C), which is selected as the optimum condition for downstream composite fabrication.

(6) Trona at 10 g/dm³ is recommended as a sustainable, locally sourced natural-alkali alternative to NaOH where the priority is environmental impact and where a modest reduction in CrI can be accepted, with the additional benefit that the milder buffered chemistry of trona inherently protects the fiber against the over-mercerization observed at high NaOH loadings.

(7) The environmental consideration for the natural alkali rests on the fact that trona is a directly obtained evaporite rather than an electrochemical product, and on the lower neutralization demand of its buffered carbonate effluent, rather than on any claim that NaOH is an expensive reagent per kilogram. Extraction of the mineral from the interdunal depressions of the Lake Chad basin is not itself impact-free, and the overland transport distance to the coconut-producing belt of southern Nigeria is substantial. No cradle-to-gate life-cycle assessment of either reagent was carried out here, and such an assessment is required before a quantitative environmental preference can be asserted.

(8) Quantitative wet-chemical fractionation of the raw and optimally treated fiber was not performed in this study. The FTIR evidence reported here establishes unambiguously which constituents each reagent removes, but it is semi-quantitative; absolute mass balances of hemicellulose and lignin removal are identified as the first priority for the follow-on work.

Taken together, these findings establish a quantitative, side-by-side basis for selecting an alkaline reagent for the mercerization of coconut coir and demonstrate that a locally sourced natural alkali can deliver thermal-stability gains comparable to those of NaOH, while requiring no industrial-scale chemical reagent. Further work is in progress to translate the optimum mercerization conditions identified here into a coir-reinforced epoxy composite and to evaluate its mechanical, physical and thermal behavior under the design conditions of a low-velocity automotive bumper energy absorber.

ACKNOWLEDGEMENTS: The authors gratefully acknowledge the technical support of the Department of Mechanical Engineering and the Central Research Laboratory of the University of Ilorin. The authors also thank the traders of Oja-

Oba market, Ilorin, for the supply of authentic Kaun bilala material used in this study. This research did not receive any specific grant from funding agencies in the public, commercial, or not-for-profit sectors.

REFERENCES

[1] S. Kaza, L. Yao, P. Bhada-Tata and F. Van Woerden, in "What a Waste 2.0: A Global Snapshot of Solid Waste Management to 2050", World Bank Publications, Washington, DC, 2018

[2] B. Yalwaji, H. John-Nwagwu and T. Sogbanmu, *Sci. Afr.*, **16**, e01220 (2022), https://doi.org/10.1016/j.sciaf.2022.e01220

[3] P. Cappelletto, F. Mongardini, B. Barberi, M. Sannibale, M. Brizzi *et al*., *Ind. Crop. Prod.*, **11**, 205 (2000), https://doi.org/10.1016/S0926-6690(99)00051-3

[4] D. Atalie, A. F. Tesema and G. K. Rotich, *J. Nat. Fibers*, **19**, 5034 (2022), https://doi.org/10.1080/15440478.2021.1875380

[5] A. Karthikeyan, K. Balamurugan and A. Kalpana, *Sci. Eng. Compos. Mater.*, **21**, 315 (2014), https://doi.org/10.1515/secm-2013-0130

[6] M. H. Hamidon, M. T. H. Sultan, A. H. Ariffin and A. U. M. Shah, *J. Mater. Res. Technol.*, **8**, 3327 (2019), https://doi.org/10.1016/j.jmrt.2019.04.012

[7] P. P. Das, A. Acharya and V. Chaudhary, "Composite Materials", CRC Press, Boca Raton, 2021, pp. 213-222

[8] D. Shelly, A. Singhal, S. Nanda and S. Banerjee, *Polym. Compos.*, **46**, S9 (2025), https://doi.org/10.1002/pc.28349

[9] J. Y. Boey, S. B. Yusoff and G. S. Tay, *Polym. Polym. Compos.*, **30**, 09673911221103600 (2022), https://doi.org/10.1177/09673911221103600

[10] A. G. Adeniyi, D. V. Onifade, J. O. Ighalo and A. S. Adeoye, *Compos. Part B Eng.*, **176**, 107305 (2019), https://doi.org/10.1016/j.compositesb.2019.107305

[11] L. Y. Mwaikambo and M. P. Ansell, *J. Appl. Polym. Sci.*, **84**, 2222 (2002), https://doi.org/10.1002/app.10460

[12] M. Chandrasekar, M. R. Ishak, S. M. Sapuan, Z. Leman and M. Jawaid, *Plast. Rubber Compos.*, **46**, 119 (2017), https://doi.org/10.1080/14658011.2017.1298208

[13] C. L. Luchese, J. B. Engel and I. C. Tessaro, *Korean J. Chem. Eng.*, **41**, 571 (2024), https://doi.org/10.1007/s11814-024-00112-6

[14] M. R. Sanjay, P. Madhu, M. Jawaid, P. Senthamaraikannan, S. Senthil *et al*., *J. Clean. Prod.*, **172**, 566 (2018), https://doi.org/10.1016/j.jclepro.2017.10.101

[15] A. Rabiu and S. A. Malami, *J. Complement. Altern. Med. Res.*, **7**, 1 (2019), https://doi.org/10.9734/jocamr/2019/v7i430109

[16] E. O'Bannon, C. Beavers and Q. Williams, *Am. Mineral.*, **99**, 1973 (2014), https://doi.org/10.2138/am-2014-4919

[17] M. Poletto, H. L. Ornaghi Junior and A. J. Zattera, *Materials*, **7**, 6105 (2014), https://doi.org/10.3390/ma7096105

[18] A. Zulkarnain, H. Wibowo and W. A. Wirawan, *Next Mater.*, **12**, 102087 (2026), https://doi.org/10.1016/j.nxmate.2026.102087

[19] H. Yang, R. Yan, H. Chen, D. H. Lee and C. Zheng, *Fuel*, **86**, 1781 (2007), https://doi.org/10.1016/j.fuel.2006.12.013

[20] M. A. S. Spinacé, C. S. Lambert, K. K. G. Fermoselli and M. A. De Paoli, *Carbohyd. Polym.*, **77**, 47 (2009), https://doi.org/10.1016/j.carbpol.2008.12.005

[21] L. Segal, J. J. Creely, A. E. Martin Jr. and C. M. Conrad, *Text. Res. J.*, **29**, 786 (1959), https://doi.org/10.1177/004051755902901003

[22] S. Nam, A. D. French, B. D. Condon and M. Concha, *Carbohyd. Polym.*, **135**, 1 (2016), https://doi.org/10.1016/j.carbpol.2015.08.035

[23] X. Fang, Y. Li, J. Zhao, J. Xu, C. Liu *et al*., *Forests*, **16**, 123 (2025), https://doi.org/10.3390/f16010123

[24] M. T. Shakthivel, K. Senthil Kumar and M. Ramesh, *Rev. Constr.*, **24**, 320 (2025), http://dx.doi.org/10.7764/rdlc.24.2.319

[25] B. D. Botan-Neto, D. Santamaria-Perez, L. Wedek, L. Bayarjargal, G. Bera *et al*., *Inorg. Chem.*, **64**, 10067 (2025), https://doi.org/10.1021/acs.inorgchem.5c00537

[26] N. Sukumar, G. R. Poongodi, H. Kalaiarasi, P. Senthamaraikannan and R. Kumar, *J. Nat. Fibers*, **22**, 2597332 (2025), https://doi.org/10.1080/15440478.2025.2597332

[27] N. A. F. Mat Nasir, C. K. Wong, J. Jamaluddin and N. Adrus, *ChemistrySelect*, **9**, e202402719 (2024), https://doi.org/10.1002/slct.202402719

[28] M. C. de Souza, I. Moroz, V. Reis, I. Cesarino and A. L. Leão, in "Coir Fiber and Its Composites: Processing, Properties and Applications", edited by M. Jawaid, Elsevier, Amsterdam, 2022, pp. 295-309

[29] M. A. Esmeraldo, A. C. H. Barreto, J. E. B. Freitas, P. B. A. Fechine, A. S. B. Sombra *et al*., *BioResources*, **5**, 2478 (2010)

[30] D. R. Naron, F. X. Collard, L. Tyhoda and J. F. Görgens, *Ind. Crop. Prod.*, **101**, 61 (2017), https://doi.org/10.1016/j.indcrop.2017.02.041

[31] N. Sweygers, D. E. C. Depuydt, A. W. Van Vuure, R. Dewil and L. Appels, *Ind. Crop. Prod.*, **186**, 115187 (2022), https://doi.org/10.1016/j.indcrop.2022.115187

[32] L. Mwaikambo and M. Ansell, *Angew. Makromol. Chem.*, **272**, 108 (1999), https://doi.org/10.1002/(SICI)1522-9505(19991201)272:1<108::AID-APMC108>3.0.CO;2-9

[33] P. Senthamaraikannan and S. Saravanakumar, *Biomass Convers. Biorefin.*, **13**, 11295 (2023), https://doi.org/10.1007/s13399-021-01858-3

[34] W. Liu, A. K. Mohanty, L. T. Drzal and M. Misra, *Polymer*, **45**, 7589 (2004), https://doi.org/10.1016/j.polymer.2004.09.009
[35] S. Park, J. O. Baker, M. E. Himmel, P. A. Parilla and D. K. Johnson, *Biotechnol*. *Biofuels*, **3**, 10 (2010), https://doi.org/10.1186/1754-6834-3-10
[36] E. Apaydın Varol and Ü. Mutlu, *Energies*, **16**, 3674 (2023), https://doi.org/10.3390/en16093674
[37] N. D. Le, M. Trogen, R. J. Varley, M. Hummel and N. Byrne, *Biomacromolecules*, **23**, 839 (2022), https://doi.org/10.1021/acs.biomac.1c01274
[38] J. Manavira, Z. Mthabela and M. O. Daramola, *Mater*. *Today Proc*., **105**, 170 (2024), https://doi.org/10.1016/j.matpr.2023.11.012
[39] I. Garcia-Herrero, M. Margallo, R. Onandía, R. Aldaco and A. Irabien, *Sci*. *Total Environ*., **580**, 147 (2017), https://doi.org/10.1016/j.scitotenv.2016.10.202
[40] B. Pham-Duc, F. Sylvestre, F. Papa, F. Frappart, C. Bouchez *et al*., *Sci*. *Rep*., **10**, 5498 (2020), https://doi.org/10.1038/s41598-020-62417-w
[41] P. J. Van Soest, J. B. Robertson and B. A. Lewis, *J. Dairy Sci*., **74**, 3583 (1991), https://doi.org/10.3168/jds.S0022-0302(91)78551-2